

Supplementary Information for

**Hollow carbon nanospheres dotted with Gd-Fe nanoparticles for
magnetic resonance and photoacoustic imaging**

Hui Zhang,^a Tianze Wu,^a Yi Chen,^a Qianqian Zhang,^a Zhenxia Chen,^a Yun Ling,^{*a,b} Yu
Jia,^a Yongtai Yang,^a Xiaofeng Liu,^a and Yaming Zhou^{*a}

^a Shanghai Key Laboratory of Molecular Catalysis and Innovative Materials,
Department of Chemistry, Fudan University, Shanghai, 200433, China.

^b Zhuhai Fudan Innovation Institute, Zhuhai, Guangdong, 519000, China.

*E-mail: yunling@fudan.edu.cn (Prof. Dr. Ling Y.)

ymzhou@fudan.edu.cn (Prof. Dr. Zhou Y. M.)

Table S1. Synthetic parameters for controlling the size and/or thickness of SiO₂@RF.

Sample	TEOS (mL)	EtOH (mL)	H ₂ O (mL)	Resorcinol (g)	HCHO (mL)	Size (nm)	Thickness (nm)
i	0.85	50	3	0.2	0.28	100±10	10
ii	0.85	50	3	0.05	0.07	140±10	10
iii	0.85	35	3	0.2	0.28	200±10	35
iv	0.85	50	3	0.4	0.56	220±10	50
v	0.85	25	3	0.2	0.28	320±10	70

Table S2. A summary information of Gd-Fe/HCSs and HCSs (100 nm).

Sample	Fe (wt %)	Gd (wt %)	r_1 ($\text{mM}^{-1}\cdot\text{s}^{-1}$)	r_2 ($\text{mM}^{-1}\cdot\text{s}^{-1}$)	BET surface area ($\text{m}^2\cdot\text{g}^{-1}$)	τ_s	η
HCSs	/	/	/	/	597	538.15	27.03%
Gd- Fe/HCSs	0.597	1.638	3.78	257.48	481	415.12	35.30%

Fig. S1 FT-IR absorption spectra of $\text{SiO}_2@\text{RF}$, $\{\text{Fe}_6\text{Gd}_6\text{P}_6\}$, $\text{SiO}_2@\text{RF}-\{\text{Fe}_6\text{Gd}_6\text{P}_6\}$, HCSs, and Gd-Fe/HCSs. (b) The as-made $\text{SiO}_2@\text{RF}$ composites are homogeneously dispersed in the EtOH solution containing $\{\text{Fe}_6\text{Gd}_6\text{P}_6\}$.

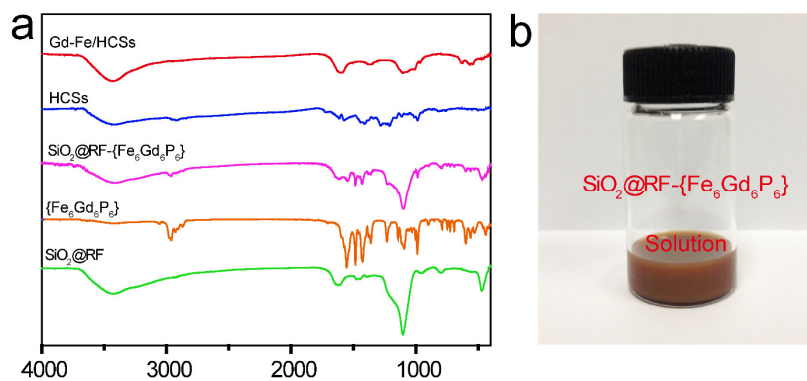


Fig. S2 (a-b) N₂ sorption isotherm of Gd-Fe/HCSs and the corresponding pore size distribution by BJH. (c-d) N₂ sorption isotherms of hollow carbon spheres (HCSs) and the corresponding pore size distribution by BJH, (e-f) N₂ sorption isotherms of core-shell SiO₂@carbon nanospheres (SiO₂@C) and the corresponding pore size distribution by BJH.

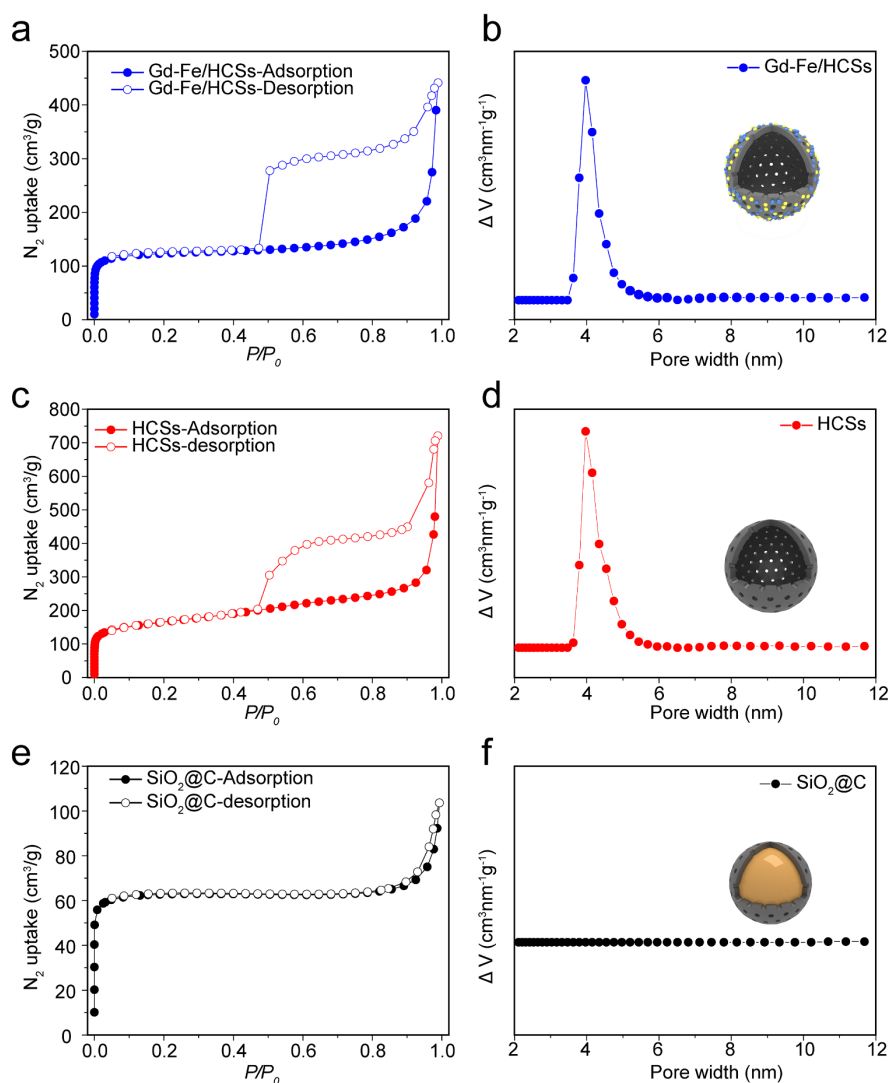


Fig. S3 Raman spectrum of Gd-Fe/HCSs and HCSs.

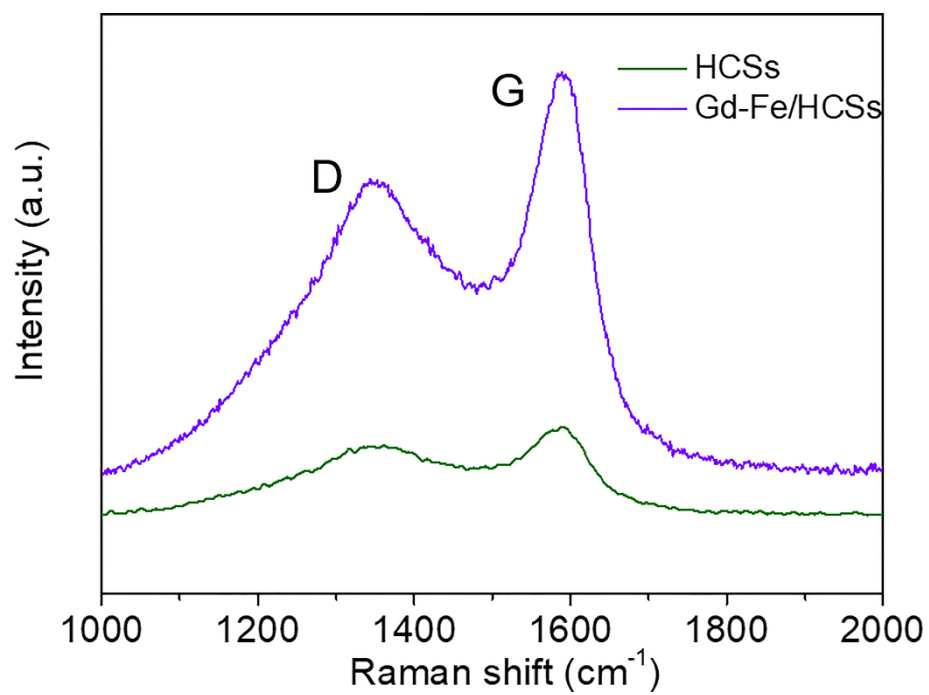


Fig. S4 (a) High-resolution TEM images. Typical lattice fringes are labeled, assigned to the characteristic lattice plane distance of GdPO₄ (red circle) and γ -Fe₂O₃ (yellow circle) (Gd-Fe), and (b) the corresponding element analysis result of Gd-Fe/HCSs, which the Gd/Fe molar ratio is measured close to 1: 1.

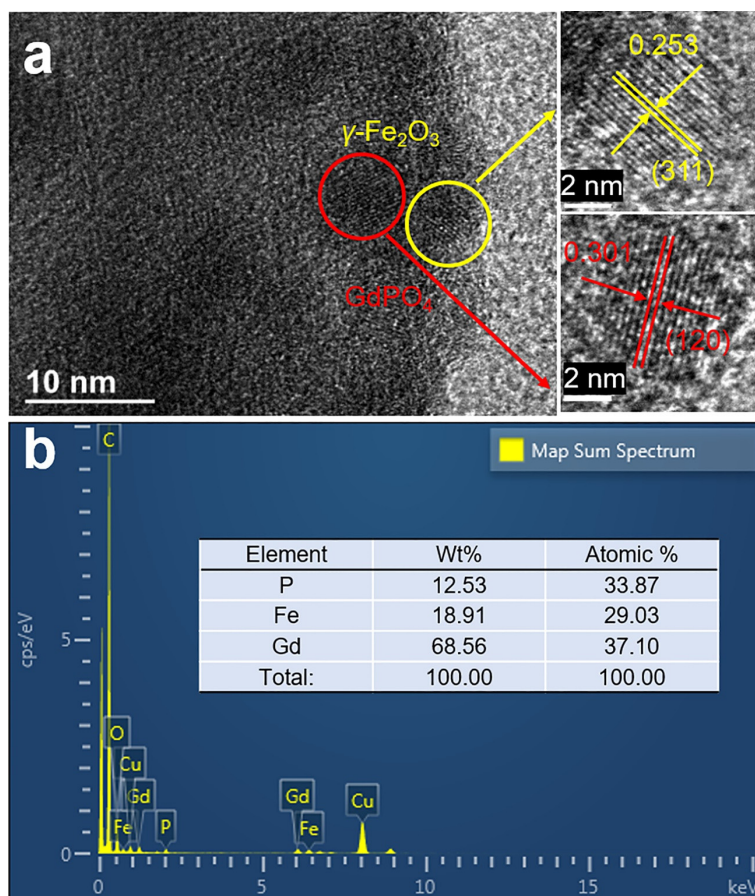


Fig. S5 PXRD patterns of Gd-Fe/HCSs, GdPO₄ (JCPDS card no. 32-0386), and γ -Fe₂O₃ (JCPDS card no. 39-1346).

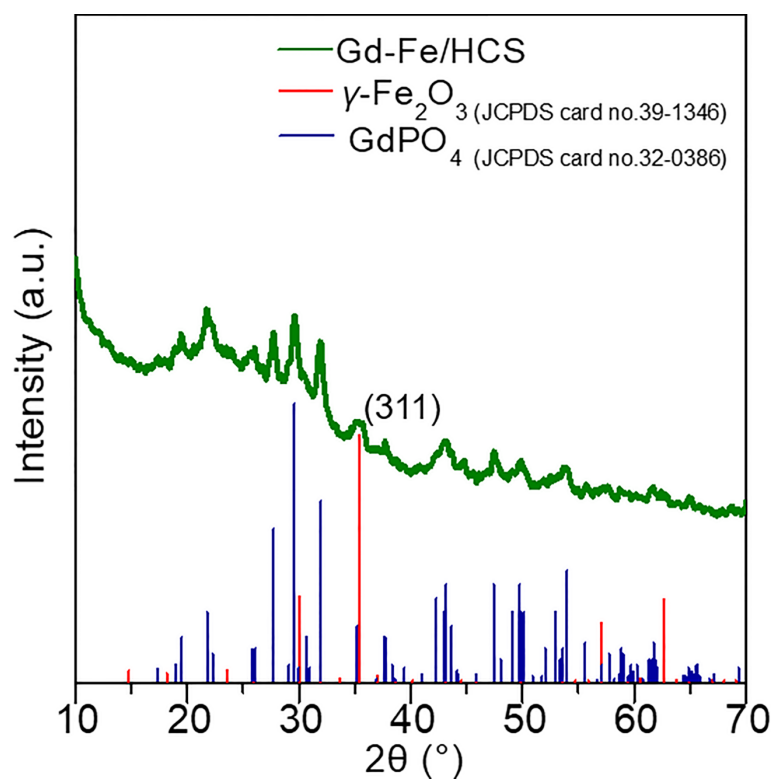


Fig. S6 (a) TEM image, (b-c) HAADF-STEM images, (d-i) overlay maps of C, O, Gd, Fe and P elements, the corresponding EDS maps of C, O, Fe, Gd, P, and EDS line profiles of the {Gd-Fe}/{SiO₂@C}.

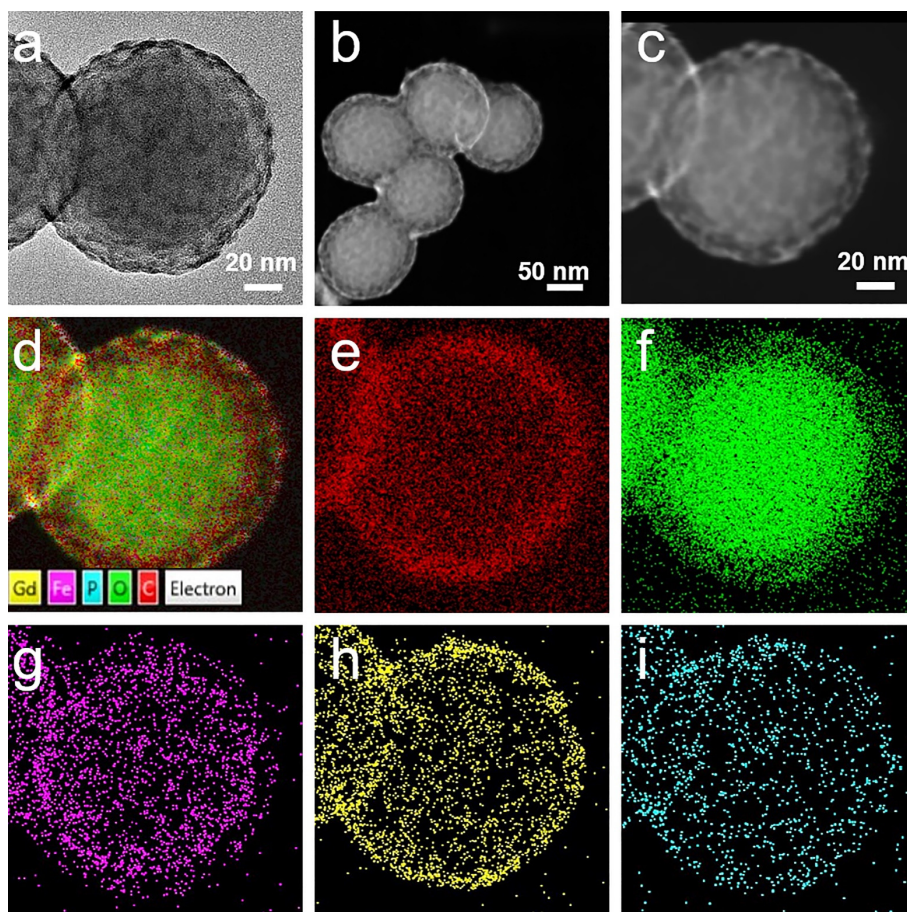


Fig. S7 (a) TEM image, (b-h) HAADF-STEM images, overlay maps of C, O, Gd, Fe and P elements, the corresponding EDS maps of C, O, Fe, Gd, P, and EDS line profiles of the Gd-Fe/HCSs.

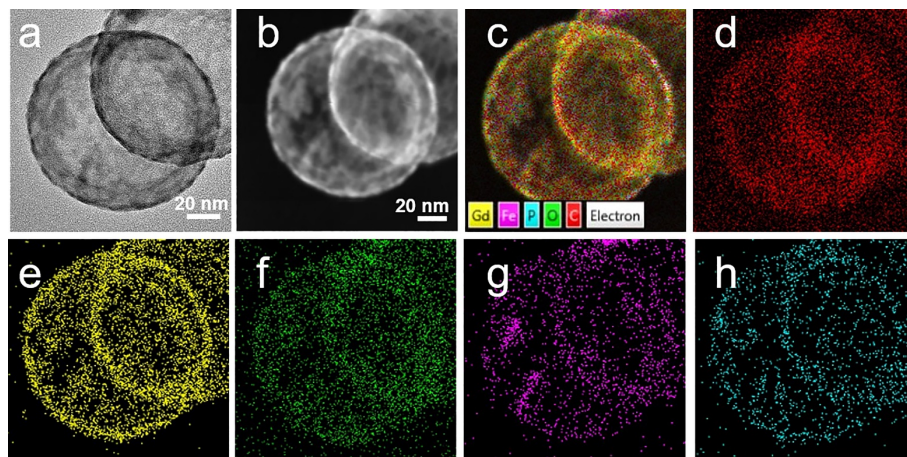


Fig. S8 A view of the different size and thickness of SiO₂@RF. (a-i) Shell thickness controlled by regulating the addition of resorcinol and HCHO. The corresponding shell thickness in a-i are 10 nm, 35 nm and 50 nm, respectively. (j-l) Size controlled by regulating the addition of EtOH. The corresponding particle sizes in j-l are 310±10 nm and the shell thickness are 70 nm.

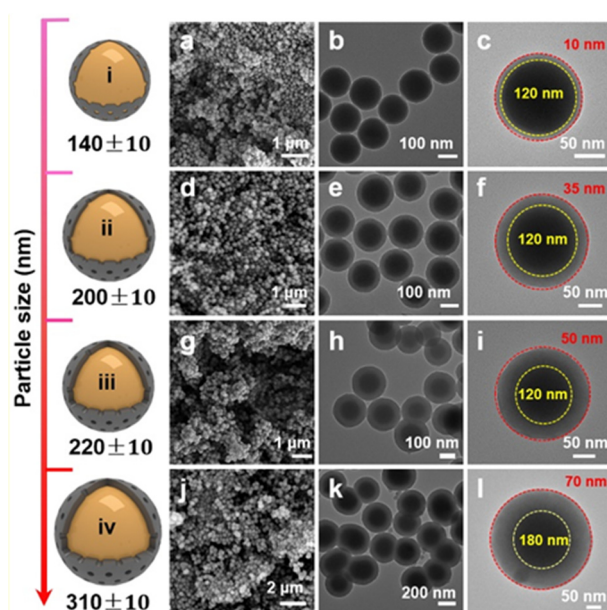


Fig. S9 TEM images of hollow carbon nanospheres with different metal loading (Gd-Fe/HCSs-n, n: the amount of $\{\text{Fe}_6\text{Gd}_6\text{P}_6\}$, n = 0 mg, 1 mg, 3 mg, 6 mg, 12 mg, 18 mg) of 100 nm: (a) HCSs, (b) Gd-Fe/HCSs-1, (c) Gd-Fe/HCSs-3, (d) Gd-Fe/HCSs-6, (e) Gd-Fe/HCSs-12, (f) Gd-Fe/HCSs-18 (100 nm).

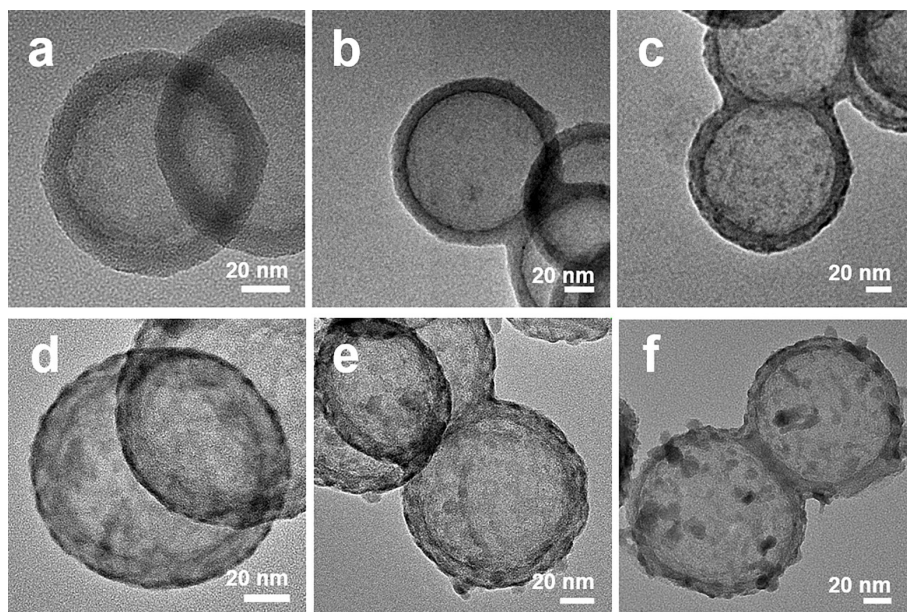


Fig. S10 TEM images of hollow carbon nanospheres with different metal loading (Gd-Fe/HCSs-n) of 320 nm: (a) HCSs, (b) Gd-Fe/HCSs-1, (c) Gd-Fe/HCSs-3, (d) Gd-Fe/HCSs-6, (e) Gd-Fe/HCSs-12, (f) Gd-Fe/HCSs-18 (320 nm).

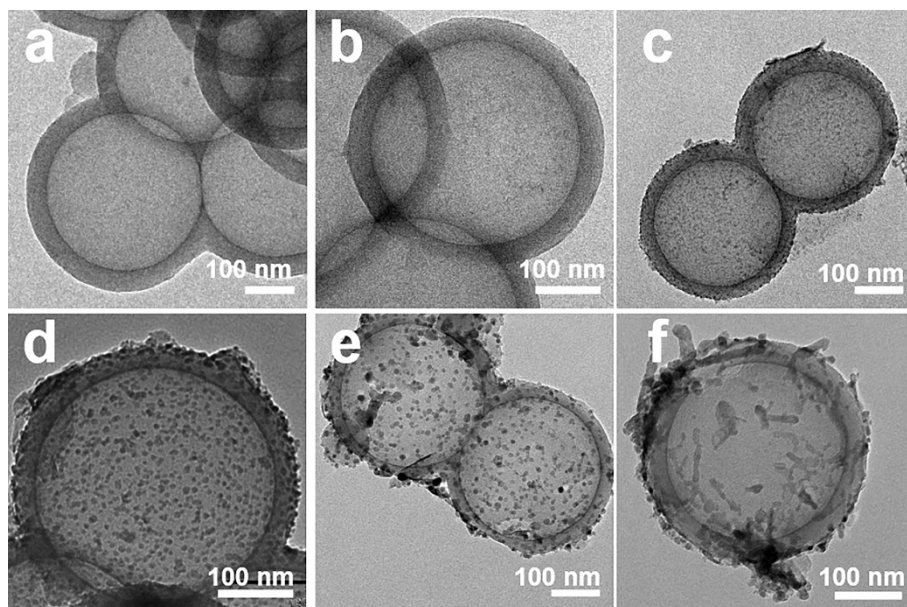


Fig. S11 PXRD patterns of Gd-Fe/HCSs-n (n= 0 mg, 1 mg, 3 mg, 6 mg, 12 mg, 18 mg) (320 nm).

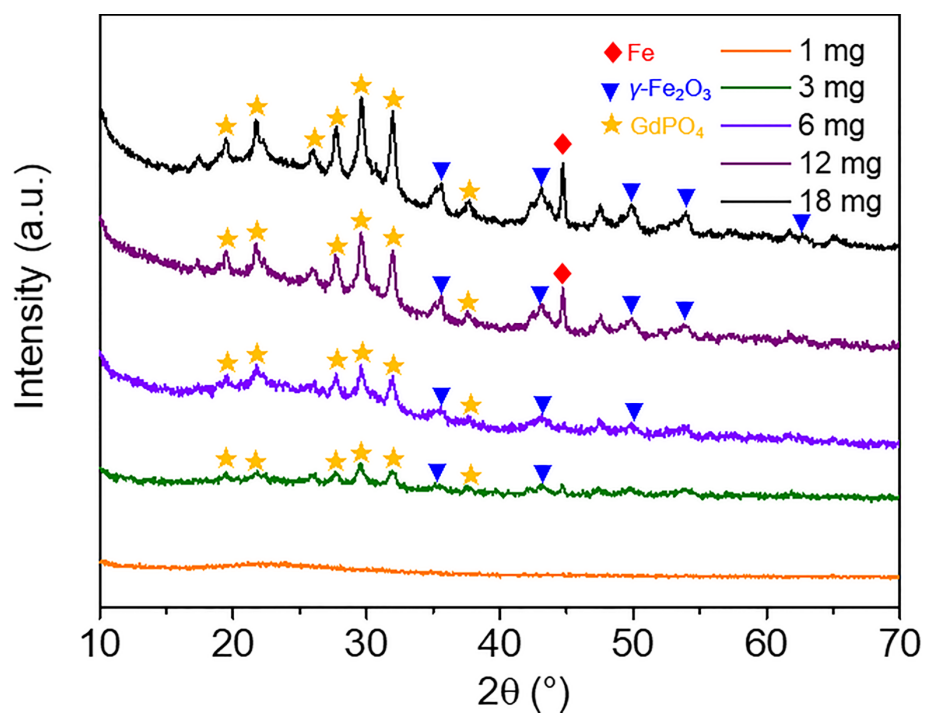
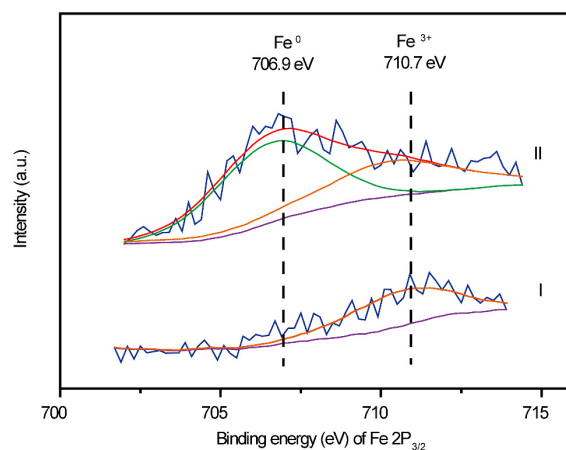


Fig. S12 Fe 2p XPS spectra of the Gd-Fe/HCSs-6 (I) and Gd-Fe/HCSs-18 (II).



As identified by TEM images (Fig. S10), the structure of hollow carbon spheres can be well retained when the dosage changes from 1 mg to 6 mg. Non-aggregation on the shell of hollow carbon spheres and good dispersion of nanoparticles indicates that GdPO₄ and γ -Fe₂O₃ nanoparticles are homogeneously dotted in the shell of HCSs. When the dosage increasing to 18 mg, the aggregation of particles can be observed (Fig. S9). The detectable peak at $2\theta = 44.6^\circ$ could be assigned the characteristic diffraction of the (110) plane of Fe⁰ (Fig. S11), which is further identified by XPS (Fig. S12). This Fe⁰ indicates the occurrence of a redox reaction between carbon and γ -Fe₂O₃.

Fig. S13 The magnetic hysteresis loop of Gd-Fe/HCSs.

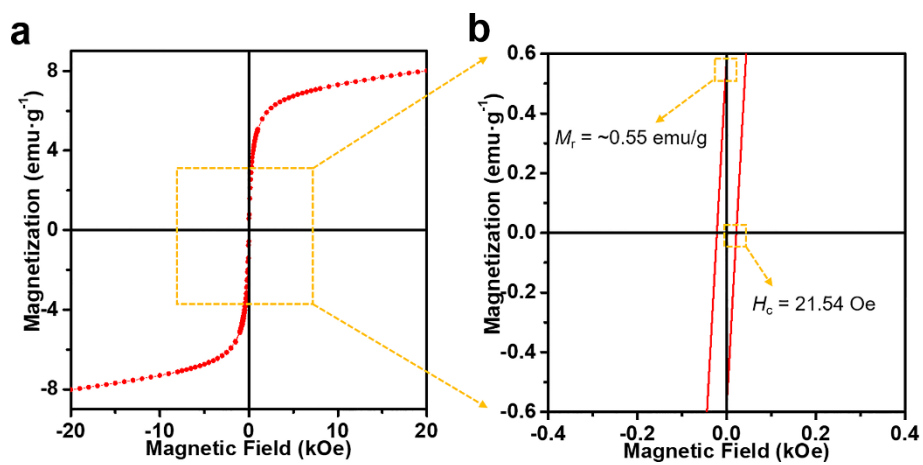


Fig. S14 Uv-vis-NIR absorbance spectra of HCSs and Gd-Fe/HCSs powders.

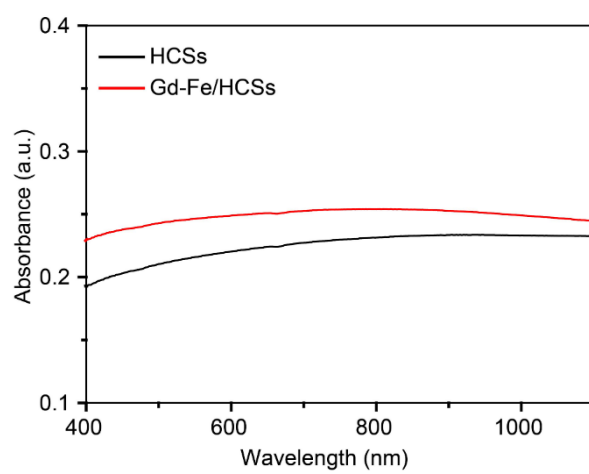


Fig. S15 (a) Uv-vis-NIR absorbance spectra of HCSs and Gd-Fe/HCSs (25, 50, and 100 $\mu\text{g}\cdot\text{mL}^{-1}$).

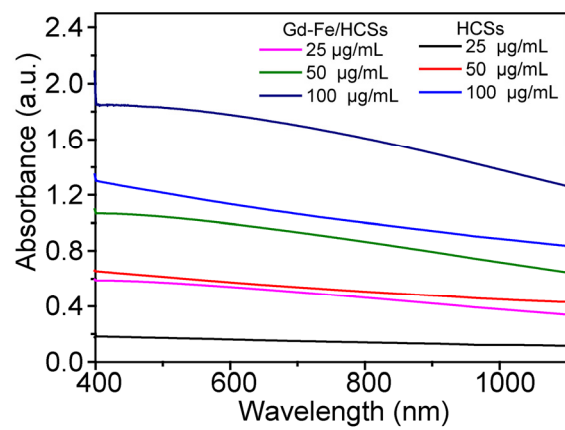


Fig. S16 The optical photograph of the infrared thermographic camera.



Fig. S17 Photothermal conversion characterizations of Gd-Fe/HCSs aqueous solution with various concentrations under 1.0 W cm^{-2} 808 nm laser irradiation for 10 min.

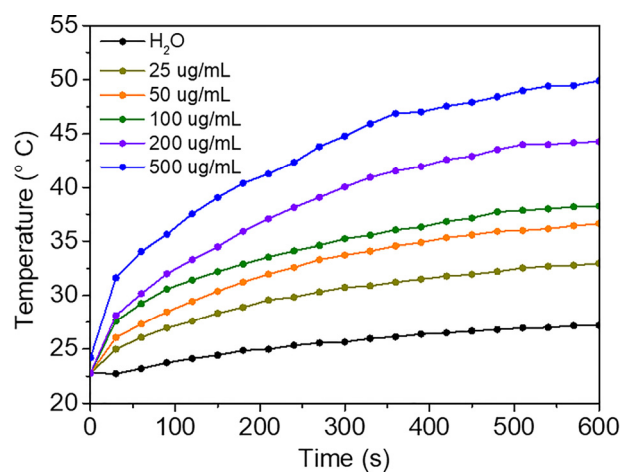


Fig. S18 Linear time data versus $-\ln(\theta)$ obtained from the cooling period of HCSs aqueous solution.

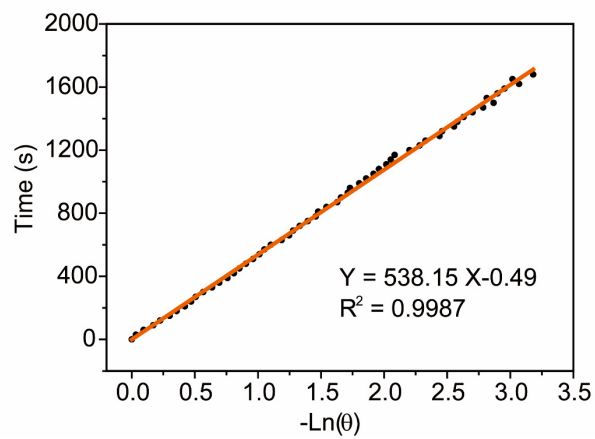


Fig. S19 The viability of HeLa cells after incubated with Gd-Fe/HCSs at different concentrations.

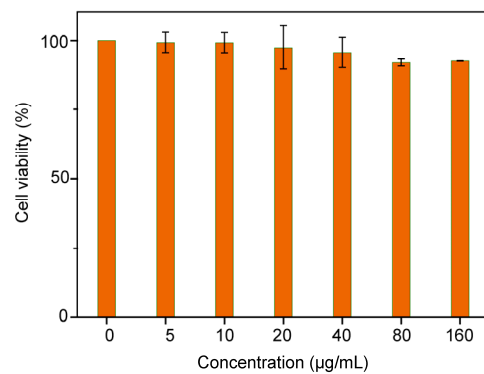


Fig. S20 The photographic images of PA images in vitro.

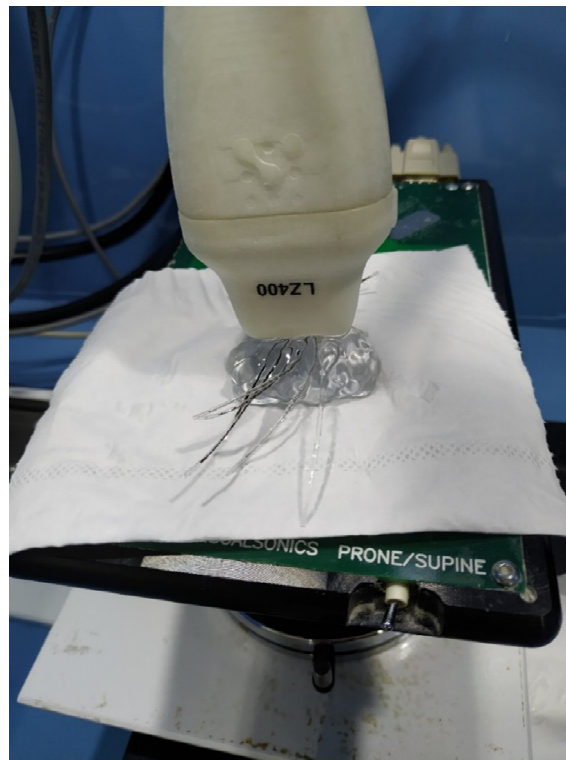


Fig. S21 (a) In vitro PA signals and (b) the corresponding PA signal intensities of HCSs with different concentrations.

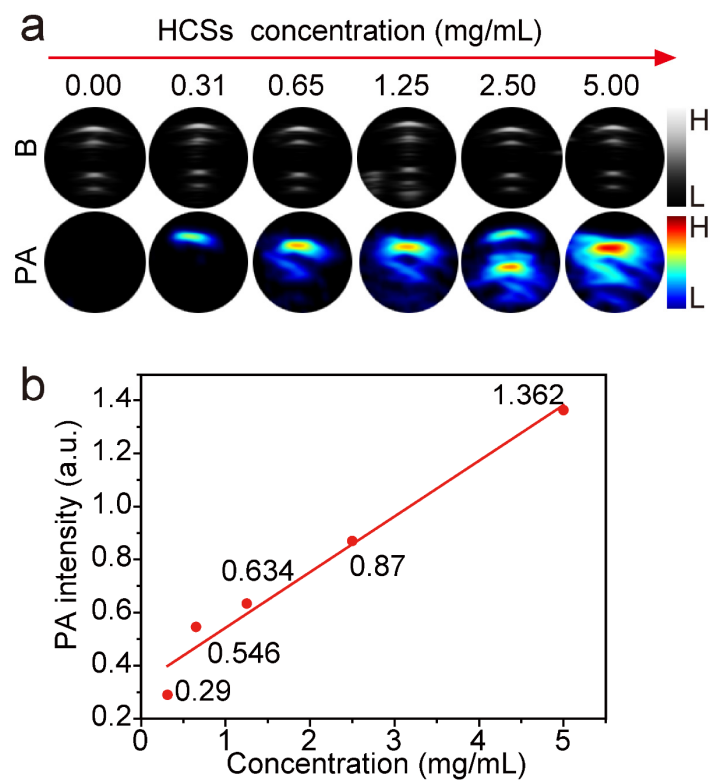


Fig. S22 (a) The optical images of the HCSs and Gd-Fe/HCSs aqueous solutions. (b) The size distribution of Gd-Fe/HCSs and (c) the zeta-potential of Gd-Fe/HCSs, and (d) the zeta-potential of HCSs.

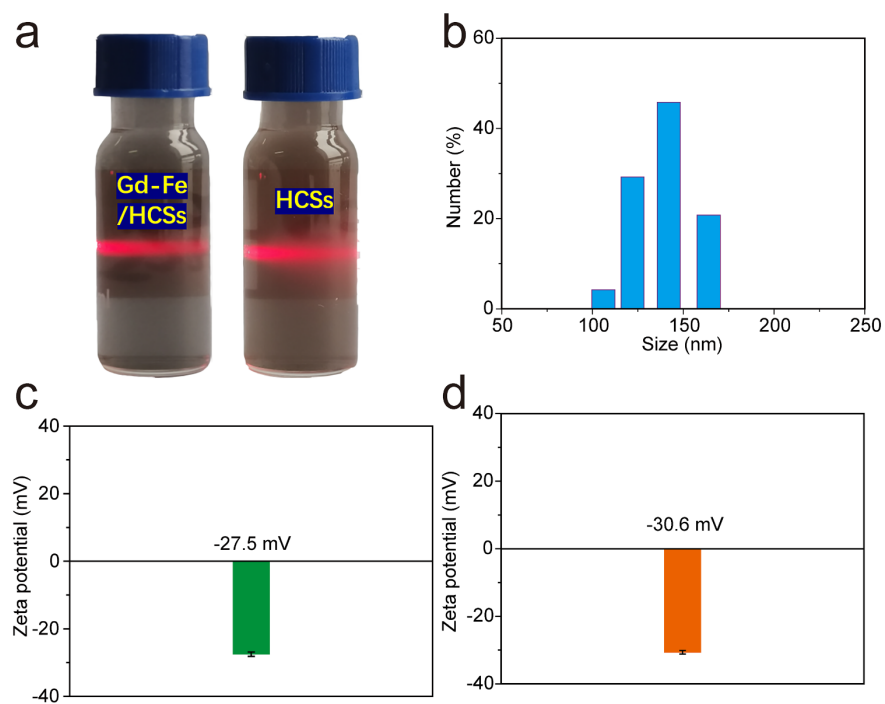


Fig. S23 (a) In vivo PA images and (b) the corresponding PA intensities of liver at different time points of HCSs (pre, 0.25 h, 1 h, 4 h, and 24 h).

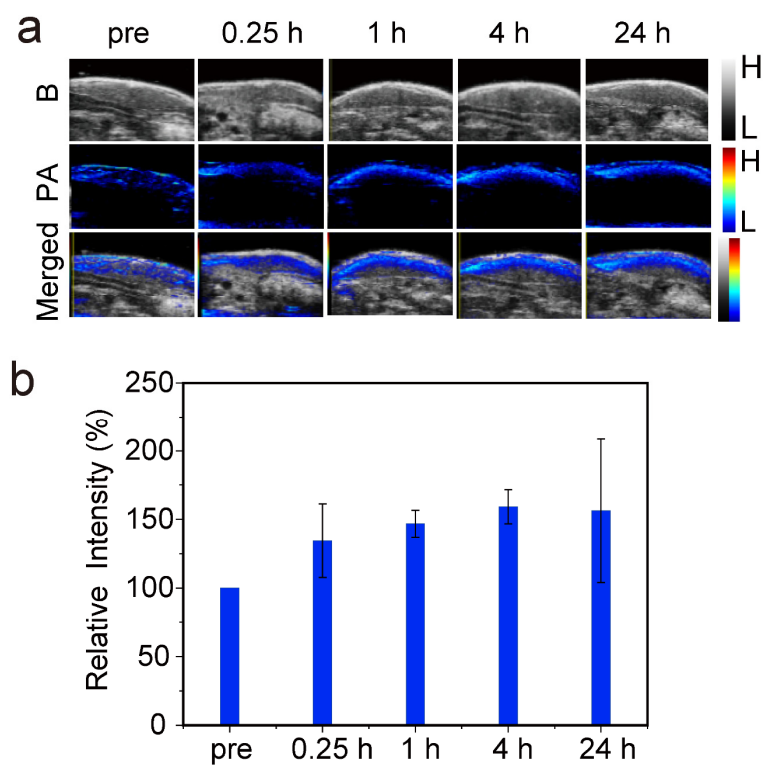


Fig. S24 Hematoxylin and eosin (H&E) images of major organs collected from mice treated with saline, and Gd-Fe/HCSs.

